
Article:
Pryor, Paul Robert orcid.org/0000-0001-9123-8329 (2017) The Salmonella effector SseJ disrupts microtubule dynamics when ectopically expressed in Normal Rat Kidney cells. PLoS ONE. ISSN 1932-6203

https://doi.org/10.1371/journal.pone.0172588

The *Salmonella* effector SseJ disrupts microtubule dynamics when ectopically expressed in Normal Rat Kidney cells.

Sally A Raines[1], Michael R. Hodgkinson[1], Adam A. Dowle[3] and Paul R Pryor[1,2*]

[1]Department of Biology and [2]Hull York Medical School, Wentworth Way, University of York. York. YO10 5DD. United Kingdom.

[3]Technology Facility, Department of Biology, Wentworth Way, University of York. York. YO10 5DD. United Kingdom

*Correspondence: paul.pryor@york.ac.uk

Short title: SseJ disrupts microtubules

Abstract

Salmonella effector protein SseJ is secreted by *Salmonella* into the host cell cytoplasm where it can then modify host cell processes. Whilst host cell small GTPase RhoA has previously been shown to activate the acyl-transferase activity of SseJ we show here an un-described effect of SseJ protein production upon microtubule dynamism. SseJ prevents microtubule collapse and this is independent of SseJ's acyl-transferase activity. We speculate that the effects of SseJ on microtubules would be mediated *via* its known interactions with the small GTPases of the Rho family.

Introduction

Salmonellae are gram-negative bacteria that can infect a wide range of hosts and in humans can cause diseases such as typhoid fever and gastroenteritis. There are ~2600 recognized *Salmonella* serovars of which over half are represented by *S. enterica* subspecies *enterica* (*S. enterica* subspecies I), constituting 99% of human clinical *Salmonella* infections. *Salmonella enterica* serovar Typhimurium (*S.* Typhimurium; the cause of gastroenteritis) uses two type III secretion systems (T3SS) to translocate pathogen effector proteins directly into the host cell's cytoplasm. (reviewed by [1]). The T3SS encoded by *Salmonella* pathogenicity island-1 (SPI-1; T3SS-1) is mostly active when extracellular *Salmonella* come into contact with a host cell and allows effector proteins to be translocated directly into the cell cytoplasm and causes the bacteria to be actively phagocytosed. Another T3SS encoded by *Salmonella* pathogenicity island-2 (SPI-2; T3SS-2) enables the bacteria to multiply intracellularly in a Salmonella

containing vacuole (SCV) by allowing further effector proteins to be translocated directly from the *Salmonella* (through the phagosomal membrane) into the host cell cytoplasm. It is unclear precisely how *Salmonella* uses its multiple T3SS effector proteins to survive intracellularly but theories range from delaying fusion with the degradative organelle the lysosome [2], though the role of the T3SS in this process is contested [3], to preventing the delivery of lysosomal hydrolases to the *Salmonella*-containing phagosomal compartment by altering mannose 6-phosphate receptor trafficking [4]. Only a finite number of intracellular membrane trafficking and signalling events can be manipulated by a pathogen and hence successful intracellular pathogens are often found to target the same host cell molecules, for instance phosphoinositides are targeted by both *Salmonellae* and *Mycobacteria* [5, 6]. Understanding how *Salmonella* survives intracellularly not only provides information about *Salmonella* pathogenesis but potentially what processes may also be targeted by other intracellular pathogens.

To understand the role of *Salmonella* T3SS effector proteins in the flow of membranes to the lysosome a rapid screen was undertaken in *Saccharomyces cerevisiae (S. cerevisiae)*. Membrane trafficking events are conserved between yeast and mammalian cells. Therefore, yeast can be used to rapidly identify any *Sallmonella* proteins that alter membrane traffic to the yeast vacuole, the equivalent of the mammalian lysosome. The screen identified the *Salmonella* virulence protein SseJ and subsequently we show a previously un-described effect of this protein on the stability of host cell microtubules. Microtubules are required for phagosome fusion [7-9] and by promoting a network of stable microtubules this can aid in phagosome fusion

with endocytic organelles enabling nutrients to be delivered to the phagosomal lumen, promoting bacterial replication.

Results

SseJ production causes membrane trafficking defects

To identify *Salmonella* proteins that can disrupt intracellular membrane trafficking, a genomic library from *Salmonella* was generated and the DNA inserted into a yeast expression vector. *S. cerevisiae* were then transformed with the plasmid library and colonies screened for a defect in the delivery of the vacuolar hydrolase, carboxypeptidase-Y (CPY), to the yeast vacuole. If there is disruption of CPY delivery to the vacuole then CPY is secreted. We assayed the secretion of a CPY-invertase fusion protein that oxidises an applied solution of o-diansidine to a brown precipitate [10]. This approach has been successfully employed to identify effector proteins of *Legionella pneumophila* [11] and *Mycobacterium tuberculosis* [12] that interfere with yeast membrane trafficking. Yeast transformed with the plasmid library were screened for CPY-Inv secretion and 8 yeast clones were found to have CPY-Inv secretion in a plasmid dependent manner. One of the clones identified a 6kb fragment of *Salmonella* chromosomal DNA containing 1 partial open reading frame (ORF) and 6 complete ORFs (Fig 1A). All of the *Salmonella* genes identified in the plasmid, were cloned and expressed individually in yeast and re-assayed for CPY secretion. Qualitative CPY-Inv secretion on agar plates showed that SseJ caused CPY secretion, though we did not analyse the protein production levels of the other 5 proteins. (Fig. 1B).

Quantitative CPY-Inv secretion from yeast in liquid culture demonstrated that SseJ dependent CPY-Inv secretion was equivalent to that in yeast lacking the CPY receptor, VPS10 (ΔVPS10; fig. 1C). There are numerous intermediate vesicles involved in delivery of CPY to the vacuole and the retrograde trafficking of the VPS10 receptor. When CPY is secreted, due to a trafficking defect, it is possible to examine the phenotype of the yeast vacuole and in some cases determine which part of the trafficking step of CPY from the Golgi to the vacuole is disrupted [13, 14]. Using the membrane dye FM4-64 to label the yeast vacuole in yeast expressing SseJ, no differences in the morphology of the vacuole were seen compared to wild-type yeast (fig. 1D). These data indicated that SseJ alone can cause a membrane trafficking defect in yeast.

SseJ production re-distributes late endocytic organelles

SseJ is one of several virulence proteins secreted by *Salmonella*'s T3SSs into the host's cytoplasm directly from the bacteria [15]. *Salmonella* strains lacking SseJ are attenuated in replication [16-19] indicating that SseJ is crucial for bacterial intracellular replication. SseJ was then expressed in mammalian cells. In this case, we used Normal Rat Kidney (NRK) cells since they show good spatial resolution between endocytic vesicles and in particular between late endosomes and lysosomes. Late-endocytic organelles are poorly resolved by light microscopy in HeLa cells, which are often used for *Salmonella* infection studies. Constitutive protein production of SseJ was found to cause cell death so myc-tagged SseJ (myc-SseJ) was expressed under the control of a metallothionein promoter allowing for inducible *sseJ* expression upon the addition of cadmium. Immunofluorescence demonstrated that myc-SseJ localises to lysosomes (Fig. 2A) as has previously been

116 reported [19]). Moreover there was a dramatic re-distribution of late endocytic
117 organelles with both late endosomes and lysosomes becoming less peri-
118 nuclear and more peripherally distributed (Fig. 2B). The *trans*-Golgi marker
119 TGN38 was observed to occupy a larger area of the cell (Fig. 2B), but in
120 general cells were flatter with an increased surface area (on average the cell
121 surface area went from 591μm^2 to 2,057μm^2 upon SseJ expression). Ectopic
122 SseJ protein production can cause globular membranous compartments
123 (GMCs) [19] and indeed when *sseJ* expression was induced for 24 h,
124 lysosomes were seen to aggregate as observed by LGP120 (rat equivalent of
125 LAMP1) staining (Fig. 2C). The metallothionein promoter regulating *sseJ*
126 expression is slightly leaky due to the presence of trace amounts of heavy
127 metals in the tissue culture media, which explains why the lysosomes are
128 partially aggregated in transfected cells before cadmium addition (Fig. 2C
129 panel b). The re-distribution of organelles is observed when the cytoskeleton
130 is perturbed [20] and indeed when the microtubule polymerisation inhibitor
131 nocodazole was added to cells, late endocytic organelles re-distributed in a
132 manner similar to that observed with SseJ expression (Fig. 2D).

133 **SseJ alters microtubule dynamics**

134 To assess whether the re-distribution of organelles was related to changes to
135 the cytoskeleton the microtubules were visualised in cells expressing SseJ or
136 a mutant SseJ (SseJ S151A). SseJ has homology to the GDSL-like lipolytic
137 enzyme family [21] and shows deacylase, phospholipase and
138 glycerophospholipid-cholesterol acyltransferase (GCAT) activity [22-24].
139 Ser151 in SseJ is the middle serine in a GDSLS motif, which is present in
140 GCAT enzymes and mutation of this residue reduces SseJ's deacylase

141 activity by 5 fold [22]. SseJ-S151A still localises to the *Salmonella* containing
142 vacuole and *Salmonella* induced filaments (Sifs) [25] are still visible in a SseJ-
143 S151A mutant strain but the bacteria show reduced virulence [22]. The
144 microtubules, in both WT and mutant-SseJ expressing cells, became
145 disorganised with no clear microtubule organising centre (MTOC; Fig. 3A). In
146 J774.2 macrophages the majority of cells don't have clear microtubules
147 emanating from a MTOC unless they have flattened out on the culture vessel
148 surface (Fig. 3B). Co-cultures of bacteria and J774.2 macrophages causes
149 the macrophages to flatten out and under these conditions the microtubule
150 network becomes more visible. However, a loss of organised microtubules,
151 emanating from a clearly defined MTOC, was seen in mouse macrophages
152 infected with WT *Salmonella* but not in cells infected with Δ*sseJ Salmonella*
153 (Fig. 3B). Typically, Δ*sseJ Salmonella* induced a four-fold increase in visible
154 microtubules emanating from the MTOC compared to control cells, but WT
155 *Salmonella* only induced a two-fold increase (Fig. 3B). Unlike nocodazole that
156 completely disrupts tubulin polymers (Fig. 2D), cells expressing SseJ still
157 show some tubulin polymers albeit in a dis-organised manner. Long-lived,
158 stable microtubules are de-tyrosinated, resulting in the exposure of a
159 glutamate residue (Glu-tubulin), and acetylated [26, 27]. Cells were then
160 examined for the presence of Glu-tubulin (Fig. 3C). In cells expressing both
161 WT and mutant SseJ protein there was a reduction in Glu-tubulin
162 immunolabelling compared to control cells. Furthermore, there was a
163 reduction in acetylated-tubulin (Fig. 3D) in WT and mutant *sseJ* expressing
164 cells. The reduction in acetylated-tubulin corresponded to the time of induction
165 of *sseJ* expression (Fig. 3E). SseJ protein production was induced with 10μM

166 cadmium and the metal can alter the cytoskeleton [28, 29] but we saw no
167 effect of cadmium on the cytoskeleton in NRK cells without *sseJ* expression
168 (all control cells in figure 3 are in the presence of 10μM cadmium chloride).
169 Together these data suggested that long-lived microtubules had been de-
170 stabilised in cells expressing SseJ, but some un-organised microtubules could
171 still be observed. When cells were transfected with a plasmid encoding GFP-
172 CLIP-170, a protein that binds to the growing ends of microtubules, and
173 visualised by live cell microscopy, no CLIP-170 movement could be observed
174 in cells expressing SseJ (supplemental movie) compared to control cells
175 (supplemental movie). Similar data were obtained with EB3-tdTomato,
176 another microtubule plus-end binding protein, and single images of EB3-
177 tdTomato transfected cells show the EB3 on the end of microtubules in control
178 cells but no visible incorporation of the EB3 onto microtubules in cells
179 expressing SseJ (Fig 3F). So whilst there was a reduction in long-lived
180 microtubules, as assessed by Glu-tubulin and acetylated-tubulin, there was no
181 dynamism in the remaining microtubules.

182 **SseJ binds both RhoA and RhoC**

183 Rho proteins are small GTPases that are primarily associated with modifying
184 the actin cytoskeleton, but they can effect cell polarity and microtubules [30].
185 SseJ can interact with both RhoA or RhoC [31, 32], with GTP-bound RhoA
186 activating SseJ's lipase activity [32]. SseJ has only previously been shown to
187 bind RhoA or RhoC separately. Large scale immunoprecipitations of SseJ
188 from cells overexpressing SseJ identified both RhoA and RhoC having bound
189 to SseJ under experimental conditions where the GTPases were in their GDP-
190 bound form (Fig. 4A), with WT and SseJ-S151A binding Rho proteins with

191 equal ability (Fig. 4B). These experiments indicate that SseJ can bind either
192 RhoA or RhoC in the presence of each other when neither protein is in a
193 limiting amount. Although we have no evidence, it is unlikely that SseJ is
194 binding both RhoA and RhoC simultaneously. Using an ELISA we found, as
195 has been reported [32], that SseJ did not increase the levels of activated
196 (GTP-bound) RhoA (Fig. 4C).

197 **Discussion**

198 In this study, we aimed to understand how *Salmonella* can survive
199 intracellularly by uncovering *Salmonella* effector molecules that can
200 manipulate membrane trafficking events. Manipulation of membrane traffic
201 may disrupt late-organelle biogenesis, including lysosomes, and therefore
202 provide conditions that enable the bacteria to replicate. We hypothesised that
203 a *Salmonella* T3SS effector molecule may manipulate membrane trafficking in
204 yeast to the same extent as mammalian cells given that the delivery of
205 molecules to the vacuole/lysosome are conserved. Using an unbiased screen
206 we identified SseJ, which is a T3SS effector protein, that caused a membrane
207 trafficking defect in yeast (Fig. 1). This is the first demonstration that SseJ
208 causes changes to membrane trafficking in eukaryotes. The powerful yeast
209 screen led us to examine the distribution of organelles in mammalian cells,
210 expecting them to be perturbed. Indeed, organelles no longer localised to the
211 MTOC (Fig. 2) and this observation could be related to changes to the
212 microtubules (Fig. 3). We further showed that SseJ can bind to both RhoA
213 and RhoC and whilst others have shown that RhoA can regulate the GCAT
214 activity of SseJ [32] this is the first report to prove the hypothesis that SseJ
215 alters the cytoskeleton [33].

How might SseJ alter the cytoskeleton? Whilst Rho proteins are well known to alter the actin cytoskeleton they can also alter the stability of microtubules via Diaphanous-related formins (DRFs) [34]. RhoA-mDia1/2 can stimulate microtubule stabilisation with an increase in Glu-tubulin, precisely how this is achieved is unknown, and it is possible that if SseJ recruits active Rho proteins to the lysosome then the RhoA-mDia1/2 balance may be disrupted leading to changes in the microtubules. Whilst we did not observe an increase in Glu-tubulin we did see static microtubules. Although the binding of SseJ to RhoA or RhoC has been documented, our data show for the first time that SseJ can bind RhoA or RhoC when both proteins are present and neither are in limited amounts i.e. SseJ does not preferentially bind RhoA and then RhoC (Fig 4). This does raise the possibility that SseJ may have differential effects through both RhoA and RhoC, with differences between RhoA, RhoB and RhoC well documented [35]. So whilst RhoA-GTP can stimulate the GCAT activity of SseJ [32], the binding of RhoC to SseJ may affect the microtubules. RhoC is reported to have a higher affinity for the kinases Rho-associated coiled-coil containing kinases (ROCK) and Citron kinase compared to RhoA [35]. MAP2/Tau proteins stabilise microtubules and inhibit depolymerisation (reviewed by [36]), an effect seen in SseJ expressing cells, and MAP2/Tau proteins can be phosphorylated by numerous kinases including ROCK [35, 37]. The effects of MAP2/Tau phosphorylation are yet to be determined, but there is a precedence for microtubule regulation by Rho proteins via DRFs and kinases such as ROCK [38]. Expression of *sseJ* before *Salmonella* infection reduces Sif formation [19], which can be explained by the fact that a dynamic cytoskeleton is required for phagosome maturation [39].

241 Additionally, whereas SseJ-S151A has reduced GCAT activity [22] the effects
242 on the microtubules are still seen in the S151A mutant suggesting that the
243 GCAT activity is separate from the microtubule effect, though we can't rule out
244 that there is still enough residual GCAT activity in cells over-expressing *sseJ*.

245 SseJ has been shown to interact indirectly with another T3SS effector
246 protein, SifA [31]. Δ*sifA* mutants escape the phagosomal vacuole but not if a
247 double *sifA sseJ* mutant is made, implying that loss of the integrity of the
248 phagosomal membrane is dependent on SseJ [19]. SifA and SseJ are
249 sufficient to cause endosome tubulation [31] and certainly SifA is required for
250 endosome tubulation [40, 41]. With SifA found to bind to RhoA, and SKIP,
251 which is a kinesin binding protein, it was hypothesised that RhoA, SseJ, SifA
252 and SKIP regulates endosome tubulation along microtubules [31]. However,
253 studies have shown that Δ*sseJ Salmonella* show endosomal tubulation
254 implying that SseJ is dispensable for endosome tubulation in a background
255 where all the other secreted effector proteins are expressed [42, 43].

256 *Salmonella* induced endosomal tubules or *Salmonella* induced
257 filaments (Sifs) are initially dynamic but become stabilised (>8h after cell
258 infection; [42] and this stabilisation could correspond to the changes that we
259 see in the dynamics of the microtubules, given that SseJ is secreted from
260 *Salmonella* within 4 h [17]. It is has been known for a long time that
261 lysosomes can form tubules [44, 45] and that microtubules regulate the
262 distribution of lysosomes [46] and their tubular morphology [7]. Although SseJ
263 is dispensable for the formation of Sifs in infected cells, SseJ may aid in
264 stabilising the Sifs that do form.. Why would this be advantageous to the
265 *Salmonella*? Endosome fusion and delivery of endocytosed material to

lysosomes can occur at the end of lysosome tubules [47] and the curvature of the membrane at the tip of a tubule is likely to be more fusogenic with endocytic vesicles compared to a larger, more-rounded phagosomal membrane [48]. By reducing microtubule de-polymerisation this allows *Salmonella* to promote tubular lysosomes (endosomal tubules), in conjunction with other proteins such as SifA, increasing fusion events with endosomal vesicles carrying in nutrients from the extracellular environment. Rho GTPases are a common target of bacterial pathogens [49, 50] and further work is required to determine whether SseJ's effect on cellular microtubules is mediated through RhoA or RhoC.

Materials and Methods

Reagents and Antibodies

Chemical reagents were of laboratory grade. Anti-c-myc (9E10) antibodies were purified from 9E10 hybridoma tissue culture supernatants (Developmental Studies Hybridoma Bank). Anti rat LGP110 (580), anti-mouse cation-independent mannose 6-phosphate receptor (MPR; 1001) and anti-rat TGN38 (2F7.1) were kind gifts from J. P. Luzio (University of Cambridge, UK). Anti α-tubulin (T-9026) was from Sigma, anti-glu-tubulin was from Synaptic Systems, anti-acetylated tubulin (D20G3), rabbit monoclonal anti-RhoA (67B9) and anti-RhoC (D40E4) were from Cell Signalling.

Yeast Strains

BHY10 and BHY11 haploid yeast strains expressing CPY-Inv [51] and BHY10 ΔVPS10::TRP1 were a kind gift from Dr. M. Seaman (University of

289 Cambridge). For the screen BHY10 and BHY11 were mated on YPD agar
290 plates, diploid yeast (BHY12) picked from SC–Lys,-Ade plates and then
291 maintained on YPD agar plates.

292 **_Salmonella_ genomic library generation**

293 Chromosomal DNA was isolated from stationary phase *Salmonella*
294 Typhimurium strain 14028 [52]. DNA was partially digested with Sau3AI for 1h
295 at 37°C. DNA was electrophoresed on a gel, and the region corresponding to
296 ≈0.8-5 kb was excised and the DNA purified. pVT-100 U [53] a gift from Dr. K.
297 Bowers (UCL, UK), was linearised with BamHI and then de-phosphorylated
298 using calf intestinal phosphatase. DNA was ligated into linearised pVT-100U
299 using T4 DNA ligase and transformed into NEB 10-beta competent *E.*
300 *coli* (High Efficiency). Ampicillin-resistant colonies (≈0.5x10^6) were scraped,
301 and plasmid DNA prepared (Qiagen midiprep).

302 **Constructs**

303 SseJ was cloned from *S.* Typhimurium DNA by PCR. Primers were used to
304 append a myc-tag to the SseJ PCR product along with 15bp regions of
305 homology to the destination vector to allow for homologous recombination
306 using In-Fusion cloning (Invitrogen). The myc-tagged SseJ DNA was inserted
307 into the HindIII restriction enzyme site of the ΔpMEP4 vector [54] by
308 homologous recombination. The S151A mutant was made by QuikChange
309 site-directed mutagenesis (Stratagene) of the myc-SseJ construct as per the
310 manufacturer's instructions.

311

312 **Invertase (Inv) assays**

313 The *Salmonella* plasmid library was transformed into BHY12 yeast [55], and
314 transformants were plated on synthetic complete medium without uracil (SC-
315 Ura) plates with 2% (w/v) fructose. Carboxypeptidase-Y-invertase (CPY-Inv)
316 assay, both quantitatively and qualitatively, is based on previous
317 methodologies [10].

318 **FM4-64 Staining**

319 1ml of log-phase yeast were pelleted and then resuspended in 50µl YPD
320 medium containing 40µM FM 4-64 (Molecular Probes). Yeast were incubated
321 at 30ºC for 15 min before the yeast were pelleted and washed with YPD
322 media. Yeast in fresh YPD were then incubated for 30 min at 30ºC. Yeast
323 were pelleted and then resuspended in 1ml of H_20 and then aliquots directly
324 visualised by confocal microscopy.

325 **Tissue culture and cell transfection**

326 All cells were cultured in Dulbecco's Modified Eagle's Medium (DMEM),
327 supplemented with 10% (v/v) FCS, 100U/L penicillin, 100mg/L streptomycin
328 and 2mM L-glutamine, in a humidified atmosphere with 5% CO_2. Cells were
329 transfected with plasmid DNA using Fugene 6 (Roche Diagnostics) as per the
330 manufacturer's instructions. ΔpMEP4 transfected cells were selected with
331 media containing 0.2 mg/ml hygromycin to generate a stable population of
332 transfected cells and individual clones were selected and assessed for SseJ
333 protein production. SseJ production was induced with 10 µM $CdCl_2$ for 16-24h
334 before analyses.

335 **J774.2 *Salmonella* infection.**

336 J774.2 cells were seeded onto glass coverslips and cultured for 48 h in
337 antibiotic-free DMEM medium supplemented with 10 % (v/v) FBS (heat
338 inactivated to 56 ºC for 30 min) and 2 mM glutamine. *Salmonellae* (WT and
339 ΔSseJ *Salmonella enterica* serovar *Typhimurium* strain 12023 were a kind gift
340 from Prof. David Holden, Imperial College London). were cultured overnight in
341 LB media with shaking at 30 ºC. An appropriate number of bacteria were
342 taken to infect J774.2 cells at an MOI (multiplicity of infection) of 10 and
343 resuspended in PBS. Bacteria were centrifuged onto cells at *80 x g* for 5 min
344 and incubated for 1 h at 37 ºC to allow phagocytosis of bacteria. Monolayers
345 were rinsed 3 times with DMEM to remove unbound bacteria, and the media
346 replaced with DMEM containing 150 µg/ml gentamycin to kill extracellular
347 bacteria. The cells were cultured for a further hour, and washed with PBS.
348 The media was then replaced with DMEM containing 10 µg/ml gentamycin,
349 and cells cultured for 24 h to allow intracellular bacteria to grow. Cells were
350 fixed with 4 % formaldehyde in PBS for 20 min at room temperature and then
351 processed for immunofluorescence.

352 **Immunofluorescence**

353 Cells were fixed with 4 % (w/v) formaldehyde in PBS for 20 min at 20ºC. Cells
354 to be immunolabelled for microtubules were rinsed with microtubule stabilising
355 buffer (MTSB; 80mM PIPES, pH 6.8, 1mM $MgCl_2$, 4mM EGTA**)** then
356 incubated in MTSB containing 0.05% (w/v) saponin (Sigma S-4521) for 1 min
357 then fixed with 2% (w/v) formaldehyde, 0.05% (w/v) glutaldehyde in MTSB for
358 20 min. Cells immunolabelled for Glu-tubulin were fixed with -20ºC MeOH for

5 min at -20ºC. All fixed cells were incubated for 10 min in 50 mM NH_4Cl in PBS followed by 10 min in 0.2 % (w/v) BSA in PBS containing 0.5% (w/v) saponin (PBS-BS). Cells were immunolabelled with primary antibodies in PBS-BS for 1h at 20ºC. Cells were rinsed 3 x 5 min with PBS-BS and then incubated with fluorescent secondary-antibodies in PBS-BS for 30 min at 20ºC. Cells were rinsed 3 x 5 min with PBS-BS before being mounted in Mowiol. Fluorescence was imaged using a Zeiss LSM510 confocal microscope. All images are maximum intensity z-projections unless otherwise stated.

Cell lysates

Lysates were generated by rinsing cells with PBS and then scraping cells into ice cold lysis buffer (150 mM NaCl, 20 mM Tris, pH 8.0, 2 mM EDTA, 0.5 % (v/v) NP-40). Lysates were left on ice for 10 min before removal of detergent insoluble material by centrifugation (16,400 *g*, 10 min, 4ºC).

Immunoprecipitation

9E10 antibody was coupled to Amino Link Plus resin (Pierce) following the manufacturer's instructions. Small scale immunoprecipitations used 20 µl of resin and 250µg of cell lysate and samples were incubated for 2 h at 4ºC with rotation. Resins were washed 3 x with lysis buffer and immunoprecipitated proteins eluted using IgG gentle elution buffer (Pierce) and analysed by SDS-PAGE. Large scale immunoprecipitations used 12 x T75 flasks and 2ml of anti-myc resin.

Mass spectroscopy

Proteins in gel bands were reduced with DTT and alkylated with iodoacetamide before digestion with modified porcine trypsin (Promega). Digests were dissolved in 4-hydroxy-α-cyano-cinnamic acid and analysed by positive-ion MALDI-MS/MS using a Bruker ultraflex III. Spectra were submitted to Mascot MS/MS ions search against the NCBI database.

RhoA activity assays

Active RhoA in cell lysates was assessed by ELISA using a RhoA activity assay (RhoA G-LISA; Cytoskeleton, Inc) as per the manufacturer's instructions.

Live cell imaging

NRK cells (WT) or expressing SseJ were transfected with either GFP-CLIP170 (kind gift of Folma Buss, University of Cambridge) or EB3-tdTomato (a kind gift from Dr Anne Straube, University of Warwick) and 24 hours later imaged on an Andor Spinning Disc Confocal Microscope. Images were collected with 200ms exposures and a 800ms delay between exposures, giving 1 frame per second.

403 **Acknowledgements**

404 We thank Gareth Evans, Nia Bryant, Jonathan Bennett and Nathalie Signoret
405 for helpful advice and for reading the manuscript.

406 **Author Contributions**

407 S.A.R. and M.H. provided technical support and carried out some of the
408 experiments. A.A.D carried out the proteomic identification of proteins. P.R.P
409 designed and carried out the majority of the research and wrote the
410 manuscript.

411

412

Figure Legends

Figure 1. Expression *of ssej* causes CPY-Inv to be mis-sorted in *Saccharomyces cerevisiae*. (A) Fragment of the *Salmonella* chromosome inserted into the yeast expression vector causing CPY-Inv secretion. (B) Qualitative CPY-Inv secretion in yeast expressing individual *Salmonella* genes identified in (A). Negative control yeast (ctrl) contain just the cloning vector (pVT-100U) and positive control yeast lack the receptor VPS10 for CPY (ΔVPS10). (C) Quantitative CPY-Inv secretion in yeast expressing *Salmonella* genes. Controls as in (B). Data are from n=3-9 (number of experiments for each condition in parentheses above each bar) and are mean ± S.D. *P<0.001 SseJ c.f. Ctrl (P>0.05 SseJ c.f. ΔVPS10). (D) Fluorescence visualisation of the yeast vacuole in wild type yeast (WT) transformed with vector (pVT-100U) alone or SseJ in pVT-100U (SseJ). Top panels DIC and bottom panels FM 4-64 fluorescence. Scale bar = 10 μm.

Figure 2. Re-distribution of late endocytic organelles in cells expressing SseJ. (A) NRK cells expressing myc-SseJ were double labelled with anti-myc (a) and anti-lysosome glycoprotein 110 (Lgp110; b) followed by fluorescently labelled secondary antibodies. Panel c is the merged image of panels a and b, co-localisation is shown by yellow. (B) Control (Ctrl) NRK cells or NRK cells expressing myc-SseJ (myc-SseJ) were immuno-labelled for the mannose 6-phosphate receptor (MPR), Lgp110 and *trans*-Golgi network 38 (TGN38) followed by fluorescently-labelled secondary antibodies to visualise the late endosomes, lysosomes and *trans*-Golgi network respectively. (C) Aggregation of Lgp110 in NRK cells expressing SseJ for 24h (a). Quantification of cells

showing aggregated lysosomes after induction of SseJ production with cadmium (Cd) (b). Expression of myc-SseJ protein -/+ Cd is shown by the western blot insert (b). (D) NRK cells were immunolabelled for microtubules (α-tubulin; a,d), lysosomes (lgp120;b,e) and late endosomes (cation-independent mannose 6-phosphate receptor; c,f) in control cells (ctrl) or after cells had been treated with 10μM nocodazole for 1h. Scale bars represent 10μm.

Figure 3. Microtubules are disrupted in cells expressing SseJ. (A) Control (Ctrl) NRK cells and cells expressing myc-SseJ (SseJ) or myc-SseJ-S151A (S151A) were fixed and the microtubules visualised using anti α-tubulin antibodies and fluorescently-labelled secondary antibodies. Bars = 10μm. (B) J774.2 mouse macrophages were either uninfected (Ctrl) or infected with WT or Δ*sseJ Salmonella* Typhimurium for 24h before fixing. The DNA (blue) was visualised using DAPI and the microtubules (red) were visualised as in A. Bars = 20μm. Quantification of the number of cells showing an organised microtubule network under each condition is shown (n=1, scoring 100 cells per condition). (C) Cells as in A were fixed and de-tyrosinated α-tubulin (Glu-tubulin) visualised by immunolabelling using anti Glu-tubulin antibodies and fluorescently-labelled secondary antibodies. Bars = 10μm. (D) Cells as in A were lysed and lysates immunoblotted for acetylated-α–tubulin (Ac-tubulin) and α-tubulin. (E) myc-SseJ production was induced in NRK cells up to 24h. Lysates were generated and western blotted for myc-SseJ, acetylated-tubulin and Rho (pan specific). (F) NRK cells (Ctrl) and those expressing *sseJ* (SseJ) were transfected with a plasmid encoding EB3-tdTomato. EB3-tdTomato was

visualised live, 24h later, on a spinning disc confocal microscope. Images represent a single time frame. Bars = 10μm.

Figure 4. SseJ binds GTPases RhoA and RhoC. (A) Anti-myc antibody was covalently attached to sepharose and myc-SseJ was immunoprecipitated from control (Ctrl) NRK cells or NRK cells expressing myc-SseJ (myc-SseJ). Proteins bound to the beads were eluted and subjected to SDS-PAGE and the gel stained with coomassie (shown). SseJ is indicated by an arrowhead. A band at ≈21kDa specifically found in the SseJ immunoprecipitation was excised and sequenced by mass spectroscopy and identified both RhoA and RhoC. Peptides identified are shown by the insert with peptides common to both RhoA and RhoC shown in bold, peptides unique to RhoA shown in blue and peptides unique to RhoC shown by red. Only a single peptide was unique to RhoC (highlighted by an asterisk). (B) Experiments as shown in A, including cells expressing myc-SseJ(S151A), were repeated and western blotted for myc, RhoA and RhoC. Western blots show 1/10th of the input before and after the immunoprecipitation and the total eluate from the immunoprecipitations. (C) The activity of RhoA was measured by ELISA, on extracts from control cells and cells expressing myc-SseJ or myc-SseJ (S151A) mutant. Data are means ± SD, n=8.

References

1. van der Heijden J, Finlay BB. Type III effector-mediated processes in Salmonella infection. Future microbiology. 2012;7(6):685-703. doi: 10.2217/fmb.12.49. PubMed PMID: 22702524.
2. Garcia-del Portillo F, Finlay BB. Targeting of Salmonella typhimurium to vesicles containing lysosomal membrane glycoproteins bypasses compartments with mannose 6-phosphate receptors. The Journal of cell biology. 1995;129(1):81-97. PubMed PMID: 7698996; PubMed Central PMCID: PMC2120372.
3. Drecktrah D, Knodler LA, Howe D, Steele-Mortimer O. Salmonella trafficking is defined by continuous dynamic interactions with the endolysosomal system. Traffic. 2007;8(3):212-25. doi: 10.1111/j.1600-0854.2006.00529.x. PubMed PMID: 17233756; PubMed Central PMCID: PMC2063589.
4. McGourty K, Thurston TL, Matthews SA, Pinaud L, Mota LJ, Holden DW. Salmonella inhibits retrograde trafficking of mannose-6-phosphate receptors and lysosome function. Science. 2012;338(6109):963-7. doi: 10.1126/science.1227037. PubMed PMID: 23162002.
5. Hernandez LD, Hueffer K, Wenk MR, Galan JE. Salmonella modulates vesicular traffic by altering phosphoinositide metabolism. Science. 2004;304(5678):1805-7. doi: 10.1126/science.1098188. PubMed PMID: 15205533.
6. Fratti RA, Backer JM, Gruenberg J, Corvera S, Deretic V. Role of phosphatidylinositol 3-kinase and Rab5 effectors in phagosomal biogenesis and mycobacterial phagosome maturation arrest. The Journal of cell biology. 2001;154(3):631-44. doi: 10.1083/jcb.200106049. PubMed PMID: 11489920; PubMed Central PMCID: PMC2196432.
7. Swanson J, Bushnell A, Silverstein SC. Tubular lysosome morphology and distribution within macrophages depend on the integrity of cytoplasmic microtubules. Proceedings of the National Academy of Sciences of the United States of America. 1987;84(7):1921-5. PubMed PMID: 3550801; PubMed Central PMCID: PMC304553.
8. Jahraus A, Storrie B, Griffiths G, Desjardins M. Evidence for retrograde traffic between terminal lysosomes and the prelysosomal/late endosome compartment. Journal of cell science. 1994;107 (Pt 1):145-57. PubMed PMID: 8175904.
9. Desjardins M, Huber LA, Parton RG, Griffiths G. Biogenesis of phagolysosomes proceeds through a sequential series of interactions with the endocytic apparatus. The Journal of cell biology. 1994;124(5):677-88. PubMed PMID: 8120091; PubMed Central PMCID: PMC2119957.
10. Darsow T, Odorizzi G, Emr SD. Invertase fusion proteins for analysis of protein trafficking in yeast. Methods in enzymology. 2000;327:95-106. PubMed PMID: 11044977.
11. Shohdy N, Efe JA, Emr SD, Shuman HA. Pathogen effector protein screening in yeast identifies Legionella factors that interfere with membrane trafficking. Proceedings of the National Academy of Sciences of the United States of America. 2005;102(13):4866-71. doi: 10.1073/pnas.0501315102. PubMed PMID: 15781869; PubMed Central PMCID: PMC555709.
12. Thi EP, Hong CJ, Sanghera G, Reiner NE. Identification of the Mycobacterium tuberculosis protein PE-PGRS62 as a novel effector that

functions to block phagosome maturation and inhibit iNOS expression. Cellular microbiology. 2013;15(5):795-808. doi: 10.1111/cmi.12073. PubMed PMID: 23167250.
13. Raymond CK, Howald-Stevenson I, Vater CA, Stevens TH. Morphological classification of the yeast vacuolar protein sorting mutants: evidence for a prevacuolar compartment in class E vps mutants. Molecular biology of the cell. 1992;3(12):1389-402. PubMed PMID: 1493335; PubMed Central PMCID: PMC275707.
14. Banta LM, Robinson JS, Klionsky DJ, Emr SD. Organelle assembly in yeast: characterization of yeast mutants defective in vacuolar biogenesis and protein sorting. The Journal of cell biology. 1988;107(4):1369-83. PubMed PMID: 3049619; PubMed Central PMCID: PMC2115260.
15. Miao EA, Miller SI. A conserved amino acid sequence directing intracellular type III secretion by Salmonella typhimurium. Proceedings of the National Academy of Sciences of the United States of America. 2000;97(13):7539-44. PubMed PMID: 10861017; PubMed Central PMCID: PMC16581.
16. Figueira R, Watson KG, Holden DW, Helaine S. Identification of salmonella pathogenicity island-2 type III secretion system effectors involved in intramacrophage replication of S. enterica serovar typhimurium: implications for rational vaccine design. mBio. 2013;4(2):e00065. doi: 10.1128/mBio.00065-13. PubMed PMID: 23592259; PubMed Central PMCID: PMC3634603.
17. Freeman JA, Ohl ME, Miller SI. The Salmonella enterica serovar typhimurium translocated effectors SseJ and SifB are targeted to the Salmonella-containing vacuole. Infection and immunity. 2003;71(1):418-27. PubMed PMID: 12496192; PubMed Central PMCID: PMC143161.
18. Lawley TD, Chan K, Thompson LJ, Kim CC, Govoni GR, Monack DM. Genome-wide screen for Salmonella genes required for long-term systemic infection of the mouse. PLoS pathogens. 2006;2(2):e11. doi: 10.1371/journal.ppat.0020011. PubMed PMID: 16518469; PubMed Central PMCID: PMC1383486.
19. Ruiz-Albert J, Yu XJ, Beuzon CR, Blakey AN, Galyov EE, Holden DW. Complementary activities of SseJ and SifA regulate dynamics of the Salmonella typhimurium vacuolar membrane. Molecular microbiology. 2002;44(3):645-61. PubMed PMID: 11994148.
20. Matteoni R, Kreis TE. Translocation and clustering of endosomes and lysosomes depends on microtubules. The Journal of cell biology. 1987;105(3):1253-65. PubMed PMID: 3308906; PubMed Central PMCID: PMCPMC2114818.
21. Upton C, Buckley JT. A new family of lipolytic enzymes? Trends in biochemical sciences. 1995;20(5):178-9. PubMed PMID: 7610479.
22. Ohlson MB, Fluhr K, Birmingham CL, Brumell JH, Miller SI. SseJ deacylase activity by Salmonella enterica serovar Typhimurium promotes virulence in mice. Infection and immunity. 2005;73(10):6249-59. doi: 10.1128/IAI.73.10.6249-6259.2005. PubMed PMID: 16177296; PubMed Central PMCID: PMC1230951.
23. Nawabi P, Catron DM, Haldar K. Esterification of cholesterol by a type III secretion effector during intracellular Salmonella infection. Molecular microbiology. 2008;68(1):173-85. doi: 10.1111/j.1365-2958.2008.06142.x. PubMed PMID: 18333886.

24. Lossi NS, Rolhion N, Magee AI, Boyle C, Holden DW. The Salmonella SPI-2 effector SseJ exhibits eukaryotic activator-dependent phospholipase A and glycerophospholipid : cholesterol acyltransferase activity. Microbiology. 2008;154(Pt 9):2680-8. doi: 10.1099/mic.0.2008/019075-0. PubMed PMID: 18757801; PubMed Central PMCID: PMC2885629.
25. Garcia-del Portillo F, Zwick MB, Leung KY, Finlay BB. Salmonella induces the formation of filamentous structures containing lysosomal membrane glycoproteins in epithelial cells. Proceedings of the National Academy of Sciences of the United States of America. 1993;90(22):10544-8. PubMed PMID: 8248143; PubMed Central PMCID: PMCPMC47813.
26. Khawaja S, Gundersen GG, Bulinski JC. Enhanced stability of microtubules enriched in detyrosinated tubulin is not a direct function of detyrosination level. The Journal of cell biology. 1988;106(1):141-9. PubMed PMID: 3276710; PubMed Central PMCID: PMC2114950.
27. Palazzo A, Ackerman B, Gundersen GG. Cell biology: Tubulin acetylation and cell motility. Nature. 2003;421(6920):230. doi: 10.1038/421230a. PubMed PMID: 12529632.
28. Li W, Zhao Y, Chou IN. Alterations in cytoskeletal protein sulfhydryls and cellular glutathione in cultured cells exposed to cadmium and nickel ions. Toxicology. 1993;77(1-2):65-79. PubMed PMID: 8442019.
29. Ledda FD, Ramoino P, Ravera S, Perino E, Bianchini P, Diaspro A, et al. Tubulin posttranslational modifications induced by cadmium in the sponge Clathrina clathrus. Aquatic toxicology. 2013;140-141:98-105. doi: 10.1016/j.aquatox.2013.05.013. PubMed PMID: 23765032.
30. Hodge RG, Ridley AJ. Regulating Rho GTPases and their regulators. Nature reviews Molecular cell biology. 2016;17(8):496-510. doi: 10.1038/nrm.2016.67. PubMed PMID: 27301673.
31. Ohlson MB, Huang Z, Alto NM, Blanc MP, Dixon JE, Chai J, et al. Structure and function of Salmonella SifA indicate that its interactions with SKIP, SseJ, and RhoA family GTPases induce endosomal tubulation. Cell host & microbe. 2008;4(5):434-46. doi: 10.1016/j.chom.2008.08.012. PubMed PMID: 18996344; PubMed Central PMCID: PMC2658612.
32. Christen M, Coye LH, Hontz JS, LaRock DL, Pfuetzner RA, Megha, et al. Activation of a bacterial virulence protein by the GTPase RhoA. Science signaling. 2009;2(95):ra71. doi: 10.1126/scisignal.2000430. PubMed PMID: 19887681.
33. Kolodziejek AM, Miller SI. Salmonella modulation of the phagosome membrane, role of SseJ. Cellular microbiology. 2015;17(3):333-41. doi: 10.1111/cmi.12420. PubMed PMID: 25620407.
34. Palazzo AF, Cook TA, Alberts AS, Gundersen GG. mDia mediates Rho-regulated formation and orientation of stable microtubules. Nature cell biology. 2001;3(8):723-9. doi: 10.1038/35087035. PubMed PMID: 11483957.
35. Wheeler AP, Ridley AJ. Why three Rho proteins? RhoA, RhoB, RhoC, and cell motility. Experimental cell research. 2004;301(1):43-9. doi: 10.1016/j.yexcr.2004.08.012. PubMed PMID: 15501444.
36. Dehmelt L, Halpain S. The MAP2/Tau family of microtubule-associated proteins. Genome biology. 2005;6(1):204. doi: 10.1186/gb-2004-6-1-204. PubMed PMID: 15642108; PubMed Central PMCID: PMC549057.
37. Castro-Alvarez JF, Gutierrez-Vargas J, Darnaudery M, Cardona-Gomez GP. ROCK inhibition prevents tau hyperphosphorylation and p25/CDK5 increase

after global cerebral ischemia. Behavioral neuroscience. 2011;125(3):465-72. doi: 10.1037/a0023167. PubMed PMID: 21517148.
38. Pan J, Lordier L, Meyran D, Rameau P, Lecluse Y, Kitchen-Goosen S, et al. The formin DIAPH1 (mDia1) regulates megakaryocyte proplatelet formation by remodeling the actin and microtubule cytoskeletons. Blood. 2014;124(26):3967-77. doi: 10.1182/blood-2013-12-544924. PubMed PMID: 25298036.
39. Harrison RE, Bucci C, Vieira OV, Schroer TA, Grinstein S. Phagosomes fuse with late endosomes and/or lysosomes by extension of membrane protrusions along microtubules: role of Rab7 and RILP. Molecular and cellular biology. 2003;23(18):6494-506. PubMed PMID: 12944476; PubMed Central PMCID: PMC193691.
40. Brumell JH, Tang P, Mills SD, Finlay BB. Characterization of Salmonella-induced filaments (Sifs) reveals a delayed interaction between Salmonella-containing vacuoles and late endocytic compartments. Traffic. 2001;2(9):643-53. PubMed PMID: 11555418.
41. Stein MA, Leung KY, Zwick M, Garcia-del Portillo F, Finlay BB. Identification of a Salmonella virulence gene required for formation of filamentous structures containing lysosomal membrane glycoproteins within epithelial cells. Molecular microbiology. 1996;20(1):151-64. PubMed PMID: 8861213.
42. Rajashekar R, Liebl D, Seitz A, Hensel M. Dynamic remodeling of the endosomal system during formation of Salmonella-induced filaments by intracellular Salmonella enterica. Traffic. 2008;9(12):2100-16. doi: 10.1111/j.1600-0854.2008.00821.x. PubMed PMID: 18817527.
43. Birmingham CL, Jiang X, Ohlson MB, Miller SI, Brumell JH. Salmonella-induced filament formation is a dynamic phenotype induced by rapidly replicating Salmonella enterica serovar typhimurium in epithelial cells. Infection and immunity. 2005;73(2):1204-8. doi: 10.1128/IAI.73.2.1204-1208.2005. PubMed PMID: 15664965; PubMed Central PMCID: PMC547014.
44. Robinson JM, Okada T, Castellot JJ, Jr., Karnovsky MJ. Unusual lysosomes in aortic smooth muscle cells: presence in living and rapidly frozen cells. The Journal of cell biology. 1986;102(5):1615-22. PubMed PMID: 3700469; PubMed Central PMCID: PMC2114221.
45. Swanson JA, Yirinec BD, Silverstein SC. Phorbol esters and horseradish peroxidase stimulate pinocytosis and redirect the flow of pinocytosed fluid in macrophages. The Journal of cell biology. 1985;100(3):851-9. PubMed PMID: 3972898; PubMed Central PMCID: PMC2113515.
46. Phaire-Washington L, Silverstein SC, Wang E. Phorbol myristate acetate stimulates microtubule and 10-nm filament extension and lysosome redistribution in mouse macrophages. The Journal of cell biology. 1980;86(2):641-55. PubMed PMID: 6893202; PubMed Central PMCID: PMC2111499.
47. Bright NA, Gratian MJ, Luzio JP. Endocytic delivery to lysosomes mediated by concurrent fusion and kissing events in living cells. Current biology : CB. 2005;15(4):360-5. doi: 10.1016/j.cub.2005.01.049. PubMed PMID: 15723798.
48. McMahon HT, Kozlov MM, Martens S. Membrane curvature in synaptic vesicle fusion and beyond. Cell. 2010;140(5):601-5. doi: 10.1016/j.cell.2010.02.017. PubMed PMID: 20211126.

678 49. Lemichez E, Aktories K. Hijacking of Rho GTPases during bacterial
679 infection. Experimental cell research. 2013;319(15):2329-36. doi:
680 10.1016/j.yexcr.2013.04.021. PubMed PMID: 23648569.
681 50. Quintero CA, Tudela JG, Damiani MT. Rho GTPases as pathogen targets:
682 Focus on curable sexually transmitted infections. Small GTPases. 2015;6(2):108-
683 18. doi: 10.4161/21541248.2014.991233. PubMed PMID: 26023809.
684 51. Horazdovsky BF, Busch GR, Emr SD. VPS21 encodes a rab5-like GTP
685 binding protein that is required for the sorting of yeast vacuolar proteins. The
686 EMBO journal. 1994;13(6):1297-309. PubMed PMID: 8137814; PubMed Central
687 PMCID: PMC394945.
688 52. Wilson K. Preparation of genomic DNA from bacteria. Current protocols in
689 molecular biology / edited by Frederick M Ausubel [et al]. 2001;Chapter 2:Unit 2
690 4. doi: 10.1002/0471142727.mb0204s56. PubMed PMID: 18265184.
691 53. Vernet T, Dignard D, Thomas DY. A family of yeast expression vectors
692 containing the phage f1 intergenic region. Gene. 1987;52(2-3):225-33. PubMed
693 PMID: 3038686.
694 54. Girotti M, Banting G. TGN38-green fluorescent protein hybrid proteins
695 expressed in stably transfected eukaryotic cells provide a tool for the real-time,
696 in vivo study of membrane traffic pathways and suggest a possible role for
697 ratTGN38. Journal of cell science. 1996;109 (Pt 12):2915-26. PubMed PMID:
698 9013339.
699 55. Gietz RD, Schiestl RH. Transforming yeast with DNA. Method Mol Cell Biol.
700 1995;5(5):255-69. PubMed PMID: WOS:A1995UH90700003.

701

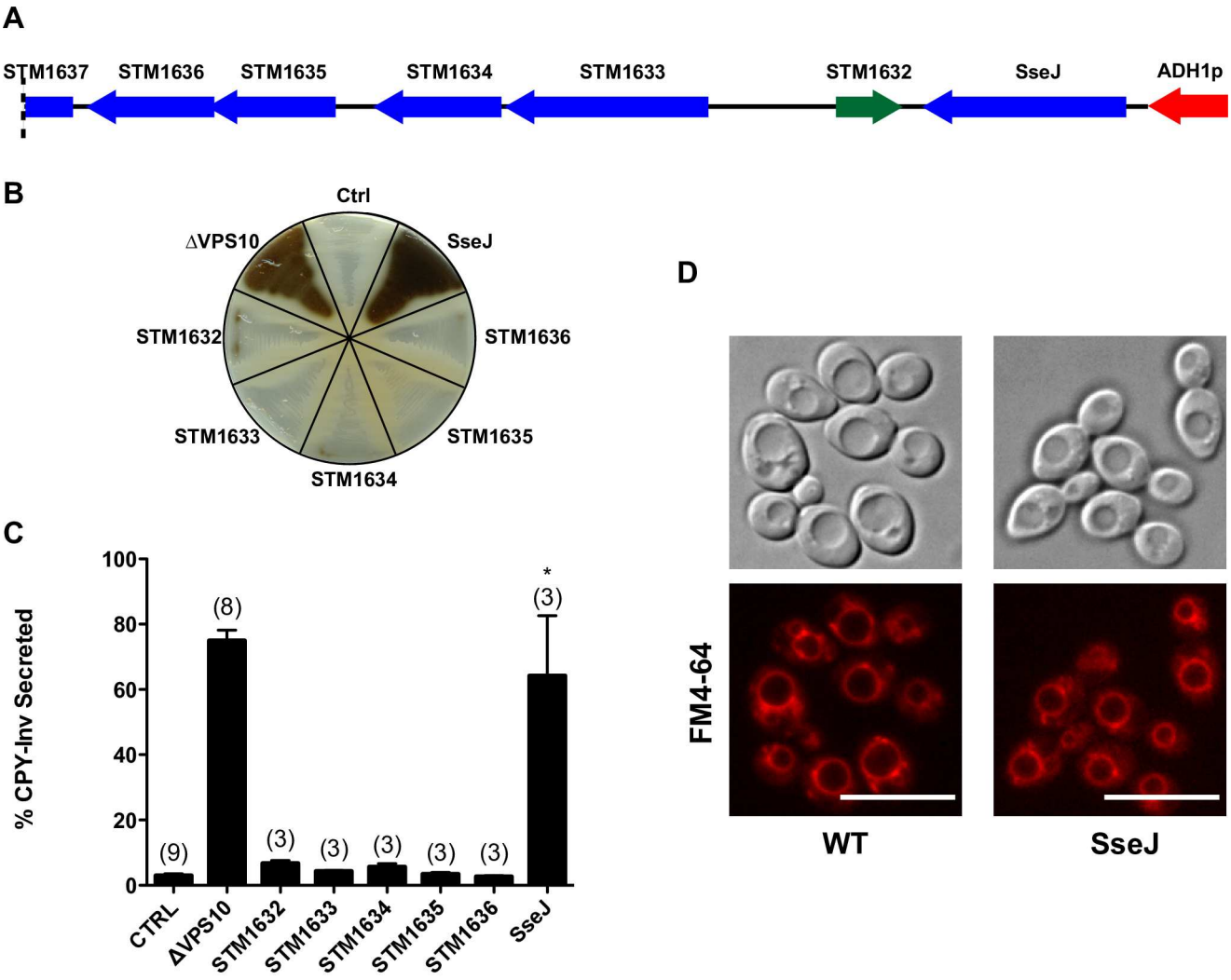
A
STM1637
STM1636
STM1635
STM1634
STM1633
STM1632
SseJ
ADH1p
B
Ctrl
ΔVPS10
SseJ
STM1632
STM1636
STM1633
STM1635
STM1634
C
% CPY-Inv Secreted
100
80
60
40
20
0
(9)
(8)
(3)
(3)
(3)
(3)
(3)
*
(3)
CTRL
ΔVPS10
STM1632
STM1633
STM1634
STM1635
STM1636
SseJ
D
FM4-64
WT
SseJ

Fig 1

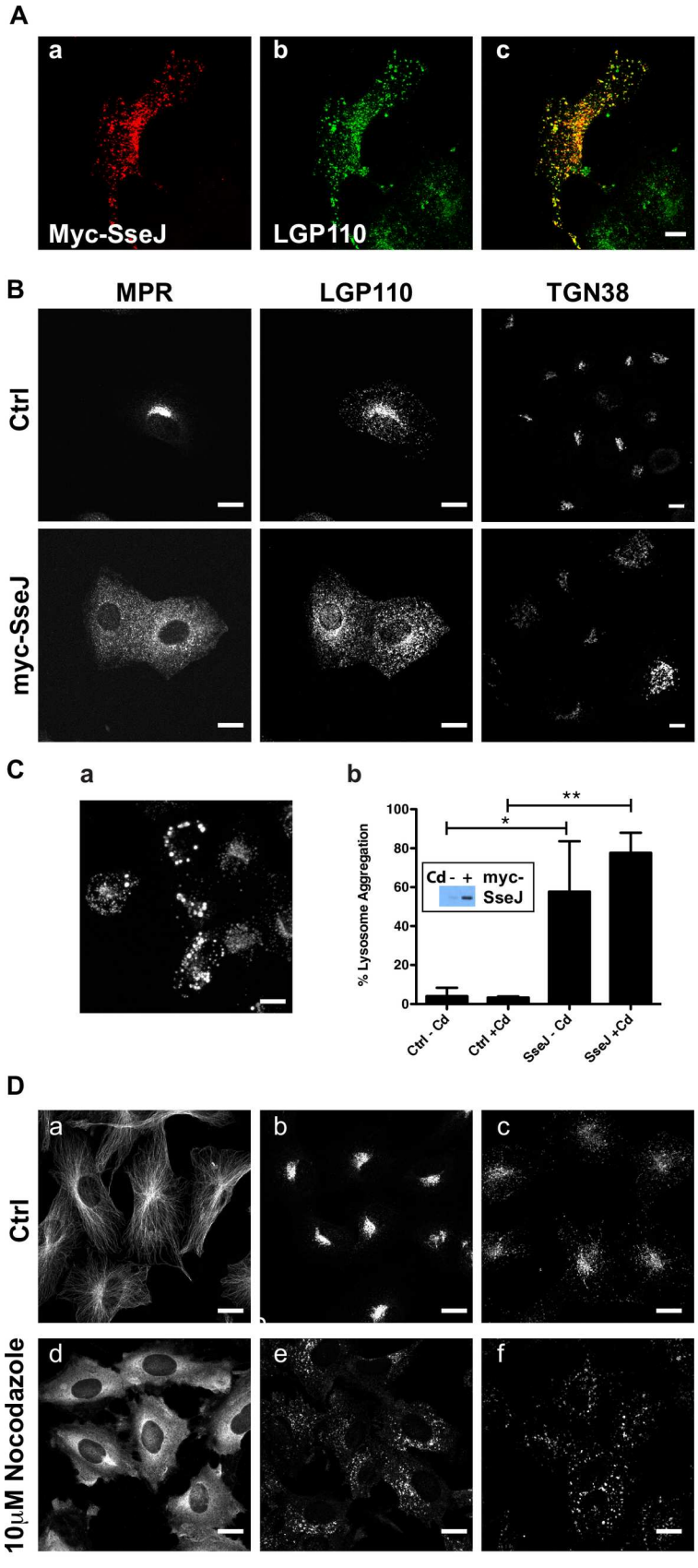
A
a
b
c
Myc-SseJ
LGP110
B
MPR
LGP110
TGN38
Ctrl
myc-SseJ
C
a
b
% Lysosome Aggregation
100
80
60
40
20
0
Cd - + myc-SseJ
*
**
Ctrl - Cd
Ctrl +Cd
SseJ - Cd
SseJ +Cd
D
a
b
c
Ctrl
d
e
f
10μM Nocodazole

Fig 2

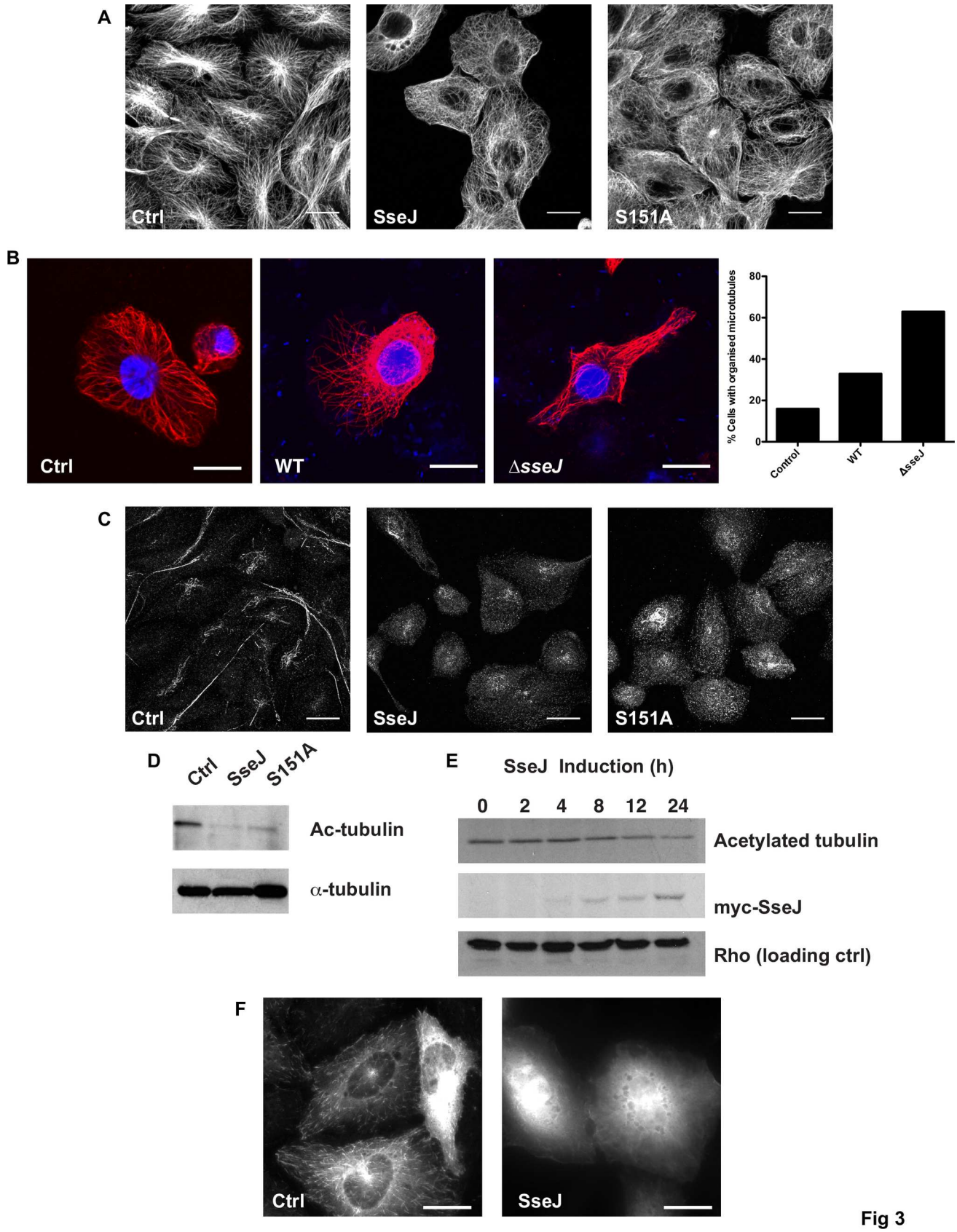
A
Ctrl
SseJ
S151A
B
Ctrl
WT
ΔsseJ
% Cells with organised microtubules
80
60
40
20
0
Control
WT
ΔsseJ
C
Ctrl
SseJ
S151A
D
Ctrl
SseJ
S151A
Ac-tubulin
α-tubulin
E
SseJ Induction (h)
0 2 4 8 12 24
Acetylated tubulin
myc-SseJ
Rho (loading ctrl)
F
Ctrl
SseJ

Fig 3

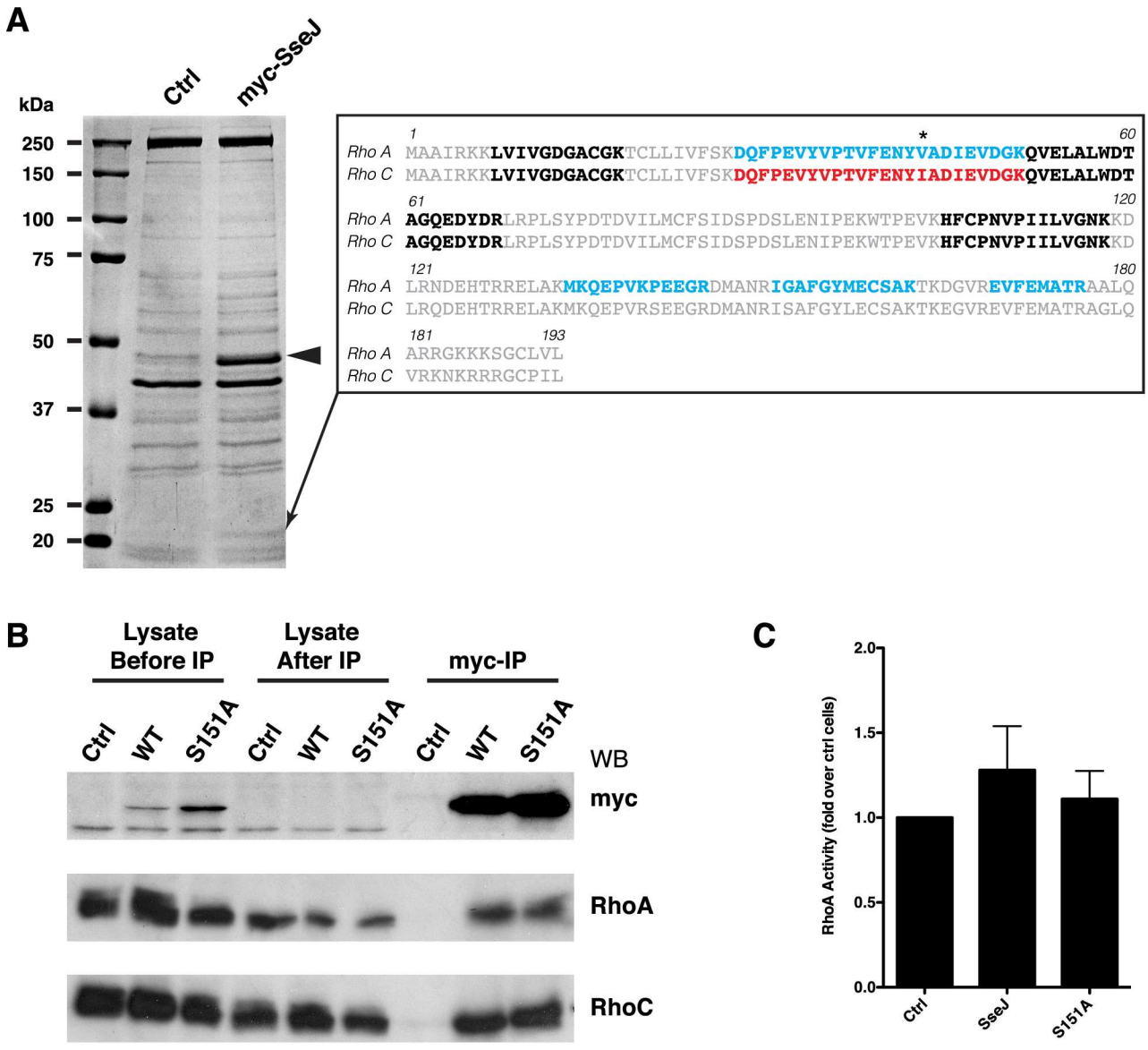
A
Ctrl
myc-SseJ
kDa
250
150
100
75
50
37
25
20
1 60
Rho A MAAIRKKLVIVGDGACGKTCLLIVFSKDQFPEVYVPTVFENYVADIEVDGKQVELALWDT
Rho C MAAIRKKLVIVGDGACGKTCLLIVFSKDQFPEVYVPTVFENYIADIEVDGKQVELALWDT
61 120
Rho A AGQEDYDRLRPLSYPDTDVILMCFSIDSPDSLENIPEKWTPEVKHFCPNVPIILVGNKKD
Rho C AGQEDYDRLRPLSYPDTDVILMCFSIDSPDSLENIPEKWTPEVKHFCPNVPIILVGNKKD
121 180
Rho A LRNDEHTRRELAKMKQEPVKPEEGRDMANRIGAFGYMECSAKTKDGVREVFEMATRAALQ
Rho C LRQDEHTRRELAKMKQEPVRSEEGRDMANRISAFGYLECSAKTKEGVREVFEMATRAGLQ
181 193
Rho A ARRGKKKSGCLVL
Rho C VRKNKRRRGCPIL
B
Lysate Before IP
Lysate After IP
myc-IP
Ctrl
WT
S151A
WB
myc
RhoA
RhoC
C
RhoA Activity (fold over ctrl cells)
2.0
1.5
1.0
0.5
0.0
Ctrl
SseJ
S151A

Fig 4